nature materials

LETTERS

PUBLISHED ONLINE: 8 FEBRUARY 2009 | DOI: 10.1038/NMAT2384

Subnanometre platinum clusters as highly active and selective catalysts for the oxidative dehydrogenation of propane

Stefan Vajda[1,2,3]*, Michael J. Pellin[4], Jeffrey P. Greeley[2], Christopher L. Marshall[1], Larry A. Curtiss[1,2,4]*, Gregory A. Ballentine[1]†, Jeffrey W. Elam[5], Stephanie Catillon-Mucherie[1], Paul C. Redfern[1], Faisal Mehmood[4] and Peter Zapol[1,2,4]

Small clusters are known to possess reactivity not observed in their bulk analogues, which can make them attractive for catalysis[1–6]. Their distinct catalytic properties are often hypothesized to result from the large fraction of under-coordinated surface atoms[7–9]. Here, we show that size-preselected $Pt_{8–10}$ clusters stabilized on high-surface-area supports are 40–100 times more active for the oxidative dehydrogenation of propane than previously studied platinum and vanadia catalysts, while at the same time maintaining high selectivity towards formation of propylene over by-products. Quantum chemical calculations indicate that under-coordination of the Pt atoms in the clusters is responsible for the surprisingly high reactivity compared with extended surfaces. We anticipate that these results will form the basis for development of a new class of catalysts by providing a route to bond-specific chemistry, ranging from energy-efficient and environmentally friendly synthesis strategies to the replacement of petrochemical feedstocks by abundant small alkanes[10,11].

The oxidative dehydrogenation (ODH) of alkanes is a reaction that is exothermic overall and is, thus, an attractive alternative to dehydrogenation of alkanes, which is an endothermic process requiring significant energy input. However, current ODH catalysts have limited activity and/or poor selectivity resulting from an inability to prevent complete oxidation[12]. The reaction scheme for propane ODH is shown in formula (1) and includes other competing pathways that lead to CO_x species.

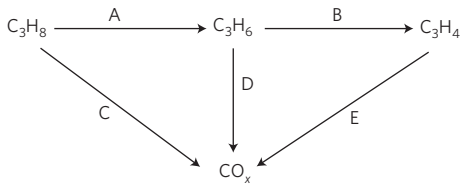

(1)

In formula (1), channel A corresponds to the pathway for propylene production and channels B, C, D and E result in less desirable products.

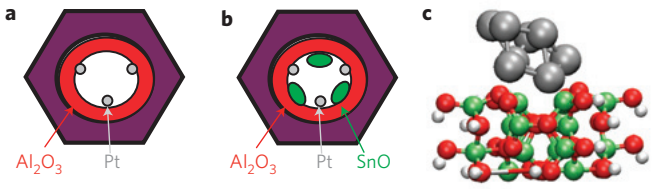

Figure 1 | Depiction of the catalytic system. a,**b**, Illustration of Pt clusters deposited in AAO membrane with ALD coating of Al_2O_3 (**a**), and with added SnO (**b**). **c**, Structure of Pt_8 cluster on an Al_2O_3 surface from density functional calculations. In this structure there are four Pt–O distances between 2.2 and 2.4 Å and the closest Pt–Al distance is 2.55 Å. See Supplementary Information for more details.

Methods for producing size-selected clusters and soft-landing them on catalytic supports are now well established[13–16]. However, testing these catalytic clusters under realistic reaction conditions requires supports on which the clusters resist sintering. Both alumina and tin oxide surfaces are known to stabilize platinum clusters[15,17]. We used atomic layer deposition (ALD) to coat porous anodized aluminium oxide (AAO, Anopore) membranes with alumina (Al_2O_3/AAO) before Pt-cluster deposition as illustrated in Fig. 1. The ALD process ensures a uniform surface chemistry[18] for the attachment of the clusters. Membranes were used in this investigation because they provide a high surface area so that high dispersions of size-selected clusters can be achieved, and catalytic tests under well-defined conditions can be carried out. The $Pt_{8–10}$ clusters were mass-selected, and a total of 900 (±135) ng Pt was soft-landed on the large pore side (~200 nm diameter) of the membrane. A pair of membranes with identical $Pt_{8–10}$ and alumina loadings were synthesized; one was left as-is and one was treated with an equivalent of two-monolayer-thick tin oxide ALD, resulting in an overcoat of the alumina support around the platinum clusters with tin oxide (SnO/Al_2O_3/AAO, Fig. 1).

Synchrotron grazing-incidence small-angle X-ray scattering studies of alumina-supported size-selected Pt clusters carried out in our laboratory[15] have provided evidence for the stability and

[1]Chemical Sciences and Engineering Division, Argonne National Laboratory, 9700 South Cass Avenue, Argonne, Illinois 60439, USA, [2]Center for Nanoscale Materials, Argonne National Laboratory, 9700 South Cass Avenue, Argonne, Illinois 60439, USA, [3]Department of Chemical Engineering, School of Engineering & Applied Science, Yale University, 9 Hillhouse Avenue, New Haven, Connecticut 06520, USA, [4]Materials Science Division, Argonne National Laboratory, 9700 South Cass Avenue, Argonne, Illinois 60439, USA, [5]Energy Systems Division, Argonne National Laboratory, 9700 South Cass Avenue, Argonne, Illinois 60439, USA. †Present Address: Max-Planck-Institut für Metallforschung, Stuttgart, Germany. *e-mail: vajda@anl.gov; curtiss@anl.gov.

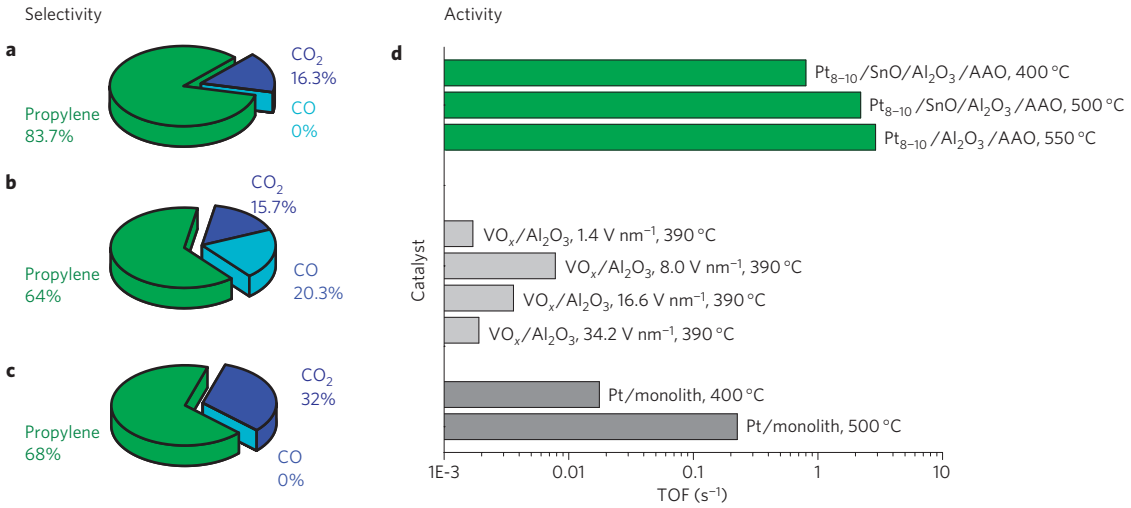

Figure 2 | Catalyst activity and selectivity. a–c, Selectivity of the Pt_{8-10}-based catalysts at various temperatures and support compositions: SnO/Al_2O_3 at 400 °C (**a**), SnO/Al_2O_3 at 500 °C (**b**) and Al_2O_3 at 550 °C (**c**). **d**, TOFs of propylene produced on the Pt_{8-10} catalysts (green) and reference ODH catalysts (grey) expressed as number of propylene molecules formed per metal atom. Pt monolith and vanadia data from refs 29 and 22, respectively. See Supplementary Information for more details.

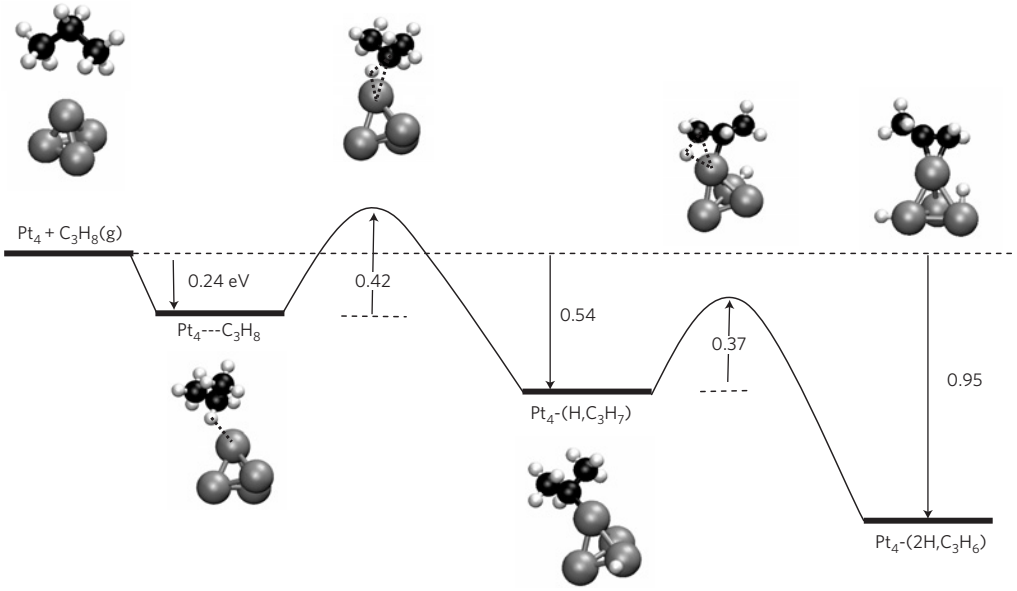

Figure 3 | Reaction path. Diagram of primary reaction steps in channel A (see formula (1)) from DFT calculations for the dehydrogenation of propane on a Pt_4 cluster leading to formation of propylene adsorbed on the cluster. Energies (in eV) of the equilibrium structures are relative to the reactants. Energy barriers for the transition state structures are relative to the preceding equilibrium structure ('true' barriers). The first barrier corresponds to breaking of the first C–H bond (on the CH_2 group) and the second barrier corresponds to breaking of the second C–H bond (on a CH_3 group). A number of other reaction steps involving hydrogen migration are not included in this diagram. The dotted lines in the structures indicate partial bonds. See Supplementary Information for more details of structures and energies and other reaction pathways.

shape of the Pt clusters. The supported clusters, similar to those used in this study, showed no evidence of agglomeration over a temperature range of 20–400 °C, and they maintained a three-dimensional structure. At the higher temperatures used in the catalytic testing in this study, there was also no evidence of any change in cluster size, as there was no change in selectivity or activity after 30 h of testing. We have also carried out density functional theory (DFT) calculations[14] to investigate the structure of a Pt_8 cluster on a θ-alumina surface. The structure (Fig. 1) indicates that the cluster maintains its three-dimensional structure, as is found in the X-ray studies. The Pt cluster forms Pt–O bonds with the surface, resulting in significant charge transfer to the cluster. The binding of the cluster to the surface (~3 eV) is consistent with the stability of the subnanometre Pt_8 clusters on alumina, but does not significantly affect the cluster's chemical reactivity (see below). In addition, we carried out calculations to investigate the stability of a positively charged Pt_8 cluster on alumina and found that it withdraws electrons from the surface and becomes negatively charged as in the case of the supported neutral cluster (see below). In a sense, these highly uniform clusters can be considered an ideal model of a single-site catalyst on technologically relevant supports, in which all active sites closely resemble each other[2,19,20].

The catalyst tests were carried out under atmospheric pressure in a flow reactor at temperatures from 400 to 550 °C by using 10 s.c.c.m. total flow of reactants in argon carrier gas with 2.63 and 2.73 mol% of oxygen and propane, respectively. The temperature range was chosen to give a direct comparison with the performance of reported Pt-and VO_x-based ODH catalysts. The measured turnover frequencies (TOFs) are shown in Fig. 2, along with the highest reported values for platinum and vanadia. The TOFs were

calculated as the number of propylene molecules produced per Pt atom per second (see Supplementary Information for details of the method of calculation). The activity and selectivity at 500 °C was unchanged over 30 h of testing.

The main finding of this study is that the activity of the Pt_{8-10} catalyst is markedly higher than any reported platinum or vanadia-based ODH catalysts. In fact, at 400 °C, the observed TOFs are 40–100 times higher than those previously reported. The product distribution (Fig. 2) indicates that selectivity for propylene over the formation of carbon oxide species is also achieved. The total conversion approaches 25% ± 4% at high temperatures. The uncertainty in the reported TOF is around 15%, determined primarily by the uncertainty in the amount of Pt loading. The uncertainty in conversion rates is given by the precision at determining the diameter of the Pt spots on the membrane using grazing-incidence small-angle X-ray scattering on poreless flat-alumina supported Pt clusters prepared under identical deposition conditions.

To understand the observed high activity of small Pt clusters for propane ODH, we carried out DFT calculations on key steps for channel A in the reaction diagram in formula (1). Channel A is the predominant channel because up to 84% of the product formed is propylene (Fig. 2). A tetrahedral Pt_4 cluster was used as a model for the Pt_{8-10} clusters because the three-coordinated Pt in this cluster is representative of the under-coordination of Pt found in the larger Pt_{8-10} clusters. The use of a free cluster model (without a substrate) is justified by the fact that the observed activity results for alumina and alumina/tin oxide substrates are similar (Fig. 2) and also by some model calculations done to investigate the substrate effect (see below).

The calculated transition states and intermediates in reaction channel A (formula (1)), leading to formation of propylene on the Pt_4 cluster, are shown in Fig. 3. The 'true' barrier to breaking of the first C–H bond is only 0.42 eV. The corresponding barrier referenced to gas-phase propane (the 'apparent' barrier) is slightly smaller, at 0.18 eV; this barrier was found to be similarly small (0.05 eV) when recalculated on a Pt_8 cluster. We note that, in spite of the small magnitude of the energetic barrier, this step will probably be rate-limiting because of the very large entropic loss, and consequentially lower pre-exponential factor, associated with propane adsorption at high temperatures on the clusters. The rest of the pathway is thermodynamically downhill to formation of propylene, which binds to Pt_4 by its π bond. Interestingly, our calculations also indicate that dissociated oxygen atoms adsorbed on the cluster[21] do not significantly affect the calculated C–H bond activities in this pathway. In the overall reaction scheme, oxygen serves as a means for removal of hydrogen as water on the basis of these calculations.

The experimental barrier for propylene formation from propane on the subnanometre Pt clusters can be estimated to provide comparison with theory. The barrier determined from the experimental data for the $Pt_{8-10}/SnO/Al_2O_3/AAO$ catalyst at 400 and 500 °C is 0.2 eV. This is consistent with the barrier found in our DFT investigation for channel A. Similarly good agreement is found when we include models for the Al_2O_3 support in our calculations. First, we considered a negatively (−1) charged Pt_4 cluster, which represents the charge transfer that occurs to the cluster when it is supported on alumina. The propane C–H reaction apparent barrier is 0.21 eV, an insignificant change from the neutral cluster. Second, we calculated the barrier for a Pt_8 cluster on a θ-alumina surface. The apparent barrier is 0.19 eV, also a small change from the result for the gas-phase Pt_8 cluster. The lack of a significant support effect is consistent with a larger binding energy per atom (~3 eV per atom) calculated for Pt_8 and Pt_4 clusters compared with the energy of each of the three Pt–alumina surface bonds (~1 eV). Although more detailed studies are needed to fully elucidate the effect of the substrate, these results are strong evidence that the support has little effect on the reaction barrier in this case. In contrast to the low C–H bond scission barrier found on Pt_4, DFT calculations for C–H bond scission in propane on a Pt(111) surface give an apparent activation barrier 1 eV larger than the corresponding barrier on Pt_4. In addition, the C–H bond cleavage barriers on a supported V_2O_5 dimer are close to 1.2 eV (ref. 22) from experiment and about 2 eV from theory for a V_2O_5 surface[23].

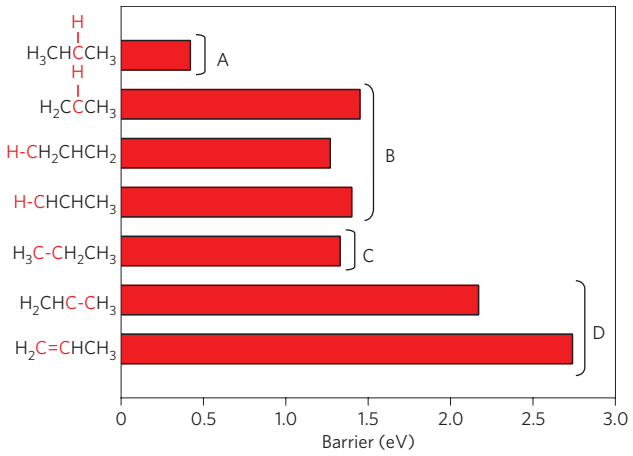

Figure 4 | Energy barriers of bond breaking. 'True' barriers for breaking C-C and C-H bonds in propane and propylene reactions on a Pt_4 cluster. Bonds that are broken are shown in red. Letters correspond to channels in formula (1). All of the barriers plotted here correspond to energies relative to the reactants (propane or propylene). In propane, the C-H bond breaking on the centre carbon (A) is favoured over a terminal carbon. In propylene C-H bond breaking all three sites (B) have similar barriers. See Supplementary Information for more details of structures and energies.

Thus, both theory and experiment lead to the conclusion that under-coordinated Pt sites in small Pt_n clusters are much more active than a Pt surface for propane ODH. This can be explained by the attractive interaction between the under-coordinated Pt and propane. The DFT calculations show that the initial adsorption complex between propane and the Pt_4 cluster (Fig. 3) results in significant charge transfer from a propane C–H bonding orbital to the cluster. This weakens the C–H bond as demonstrated by its lengthening and a concomitant lowering of the C–H vibrational frequency by ~500 cm^{-1}. In contrast, propane is very weakly adsorbed on a Pt(111) surface with essentially no C–H bond lengthening or charge transfer owing to higher coordination of the surface Pt atoms.

The observed product distribution, favouring propylene formation over CO_x (84% versus 16% at 400 °C—Fig. 2), suggests that C–C or C=C cleavage on the Pt clusters is less favourable than is C–H cleavage. Calculated activation barriers for various such reactions (Fig. 4) confirm this conclusion. For example, the barrier for breaking a C–C bond in propane is greater than 1 eV. In addition, propylene itself is relatively unreactive; the barriers for C–C and C=C breaking range from 2.2–2.7 eV. In addition, the barrier to break a C–H bond in the methyl group of adsorbed propylene is quite large (1.27 eV). The relatively large magnitude of this barrier is due to the considerable structural rearrangement required for the methyl group in propylene to come in contact with the Pt_4 cluster. These results, taken together, indicate that propylene will be easily formed, but other by-products, such as allene and CO_x, will not form easily.

The calculated selectivity trends can be understood from the electronic structures of the C–C and C–H bond-breaking transition states. The larger barriers observed for C–C versus C–H bond breaking are probably due to the sp^3 directionality of the orbitals on C compared with the spherical nature of the orbital on hydrogen,

which results in poorer overlap between the adsorbate and the reaction site orbitals in the transition state for breaking the C–C bond compared with that for the C–H bond. This argument has been put forward by Blomberg *et al.* for other surface reactions[24]. Computations indicate that CH_4 (ref. 25) and H_2 (ref. 26) have a small barrier and no barrier, respectively, for dissociation on a Pt_4 cluster, which supports the overlap explanation.

To our knowledge, the work reported here is the first investigation of size-preselected Pt clusters under realistic high-temperature catalytic conditions. It has revealed a very high activity of subnanometre Pt-cluster-based catalysts for the ODH of propane to propylene. Combined with quantum chemical studies, this work has shown that the high activity is due to the under-coordination of the Pt in the clusters and that the clusters favour the scission of C–H bonds relative to C–C or C=C bonds. Some recent work in our laboratory demonstrates that small gold clusters (Au_{6-10}) are highly active for propylene epoxidation, thus providing further evidence for the unique catalytic properties of subnanometre clusters[27]. In the future, size-selected clusters stabilized on appropriate supports with uniform surface chemistry hold great promise for design of new catalytic materials. It will be a challenging task to scale up the production of size-selected clusters by more conventional chemical methods, but there are very encouraging efforts suggesting that this will ultimately be possible[2,3].

Methods

Production of narrow cluster size distributions. The clusters emerging from the continuous beam cluster source possess identical velocity. Owing to the variation in their kinetic energy with size, in addition to the single mass selection on a quadrupole mass filter, narrow distributions of clusters with one to four sizes can be isolated using a quadrupole deflector operated in energy filter mode.

Determination of the fraction of clusters in the pores acting as active catalysts. As only 10.5% of the facing area of the membrane was exposed to clusters, and to the propane feed, a multiplication factor of 9.5 is applied to obtain the corrected propane conversion rate on the Pt-cluster-coated fraction of the AAO membrane. By calculating the relative pore opening area to the total surface area of the membrane, 28% of the Pt_{8-10} particles, corresponding to 252 ng of Pt metal, enter the pores. The rest forms metallic platinum on the face of the AAO membrane as confirmed by X-ray photoemission spectroscopy. Metallic Pt is known to possess orders of magnitude lower TOFs for ODH of propane[28]. Thus, 252 ng of Pt was used for the calculation of the TOFs.

Activation barrier calculation from the experimental data. Using Arrhenius law and assuming that the conversion rate is roughly proportional to the fraction of activated C–H bonds, an estimate was obtained of the activation barrier from two available experimental values for $Pt_{8-10}/SnO/Al_2O_3/AAO$ catalyst at different temperatures.

Theoretical methods. The calculations were done using the B3LYP functional with the LANL2DZ basis set for Pt and 6-31G* for Al, C, H and O. The Pt(111) results were obtained with plane-wave calculations using the RPBE functional. See Supplementary Information for more details.

Received 21 July 2008; accepted 12 January 2009; published online 8 February 2009

References

1. Xu, Z. *et al.* Size-dependent catalytic activity of supported metal clusters. *Nature* **372**, 346–348 (1994).
2. Gates, B. C. Supported metal clusters: Synthesis, structure, and catalysis. *Chem. Rev.* **95**, 511–522 (1995).
3. Argo, A. M., Odzak, J. F., Lai, F. S. & Gates, B. C. Observation of ligand effects during alkene hydrogenation catalysed by supported metal clusters. *Nature* **415**, 623–623 (2002).
4. Fu, Q., Saltsburg, H. & Flytzani-Stephanopoulos, M. Active Nonmetallic Au and Pt species on ceria-based water-gas shift catalysts. *Science* **301**, 935–938 (2003).
5. Campbell, C. T. The active site in nanoparticle gold catalysis. *Science* **306**, 234–235 (2004).
6. Chen, M. S. & Goodman, D. W. The structure of catalytically active gold on titania. *Science* **306**, 252–255 (2004).
7. Lemire, C., Meyer, R., Shaikhutdinov, S. & Freund, H.-J. Do quantum size effects control CO adsorption on gold nanoparticles? *Angew. Chem. Int. Ed.* **43**, 118–121 (2004).
8. Wei, J. & Iglesia, E. Mechanism and site requirements for activation and chemical conversion of methane on supported Pt clusters and turnover rate comparisons among noble metals. *J. Phys. Chem. B* **108**, 4094–4103 (2004).
9. Hvolbaek, B. *et al.* Catalytic activity of Au nanoparticles. *Nano Today* **2**, 14–18 (2007).
10. Hutchings, G. J., Scurrell, M. S. & Woodhouse, J. R. Oxidative coupling of methane using oxide catalysts. *Chem. Soc. Rev.* **18**, 251–283 (1989).
11. Labinger, J. A. & Bercaw, J. E. Understanding and exploiting C–H bond activation. *Nature* **417**, 507–509 (2002).
12. Cavani, F., Ballarini, N. & Cericola, A. Oxidative dehydrogenation of ethane and propane: How far from commercial implementation? *Catal. Today* **127**, 113–131 (2007).
13. Benz, L. *et al.* Landing of size-selected Ag_n^+ clusters on single crystal TiO_2 (110)-(1 × 1) surfaces at room temperature. *J. Chem. Phys.* **122**, 081102 (2005).
14. Lee, S., Fan, C., Wu, T. & Anderson, S. L. CO oxidation on Au_n/TiO_2 catalysts produced by size-selected cluster deposition. *J. Am. Chem. Soc.* **126**, 5682–5683 (2004).
15. Winans, R. E. *et al.* Reactivity of supported platinum nanoclusters studied by *in situ* GISAXS: Clusters stability under hydrogen. *Top. Catal.* **39**, 145–149 (2006).
16. Yoon, B. *et al.* Charging effects on bonding and catalyzed oxidation of CO on Au_8 clusters on MgO. *Science* **307**, 403–407 (2005).
17. Sadykov, V. A. *et al.* Oxidative dehydrogenation of propane over monoliths at short contact times. *Catal. Today* **61**, 93–99 (2000).
18. Pellin, M. J. *et al.* Mesoporous catalytic membranes: Synthetic control of pore size and wall composition. *Catal. Lett.* **102**, 127–130 (2005).
19. Bell, A. T. The impact of nanoscience on heterogeneous catalysis. *Science* **299**, 1688–1691 (2003).
20. Somorjai, G. A., Contreras, A. M., Montano, M. & Rioux, R. M. Cluster chemistry and dynamics special feature: Clusters, surfaces, and catalysis. *Proc. Natl Acad. Sci.* **103**, 10577–10583 (2006).
21. Xu, Y., Shelton, W. A. & Schneider, W. F. Thermodynamic equilibrium compositions, structures, and reaction energies of Pt_xO_y ($x = 1$–3) clusters predicted from first principles. *J. Phys. Chem. B* **110**, 16591–16599 (2006).
22. Argyle, M. D., Chen, K., Bell, A. T. & Iglesia, E. Effect of catalyst structure on oxidative dehydrogenation of ethane and propane on alumina-supported vanadia. *J. Catal.* **208**, 139–149 (2002).
23. Redfern, P. C. *et al.* Quantum chemical study of mechanisms for oxidative dehydrogenation of propane on vanadium oxide. *J. Phys. Chem. B* **110**, 8363–8371 (2006).
24. Blomberg, M. R. A., Siegbahn, P. E. M., Nagashima, U. & Wennerberg, J. Theoretical study of the activation of alkane C–H and C–C bonds by different transition metals. *J. Am. Chem. Soc.* **113**, 424–433 (1991).
25. Xiao, L. & Wang, L. Methane activation on Pt and Pt_4: A density functional theory study. *J. Phys. Chem. B* **111**, 1657–1663 (2007).
26. Cruz, A., Bertin, V., Poulain, E., Benitez, J. I. & Castillo, S. Theoretical study of the H_2 reaction with a Pt_4 (111) cluster. *J. Chem. Phys.* **120**, 6222–6225 (2004).
27. Lee, S. *et al.* Selective propene epoxidation on immobilized Au_{6-10} clusters: The effect of hydrogen and water on selectivity and activity. *Angew. Chem. Int. Ed.* (in the press, 2008) <http://dx.doi.org/10.1002/anie.200804154>.
28. Yu, C., Xu, H., Ge, Q. & Li, W. Properties of the metallic phase of zinc-doped platinum catalysts for propane dehydrogenation. *J. Mol. Catal. A* **266**, 80–87 (2007).
29. Silberova, B., Fathi, M. & Holmen, A. Oxidative dehydrogenation of ethane and propane at short contact time. *Appl. Catal. A* **276**, 17–28 (2004).

Acknowledgements

The work at Argonne National Laboratory was supported by the US Department of Energy, BES-Chemical Sciences, BES-Materials Sciences, and BES-Scientific User Facilities under Contract DE-AC-02-06CH11357 with UChicago Argonne, LLC, Operator of Argonne National Laboratory. S.V. gratefully acknowledges the support by the Air Force Office of Scientific Research. We acknowledge grants of computer time at the Laboratory Computing Resource Center (LCRC) at Argonne National Laboratory, the National Energy Research Scientific Computing Center (NERSC) at Lawrence Berkeley National Laboratory and the Molecular Science Computing Facility (MSCF) at Pacific Northwest National Laboratory. The authors are indebted to E. Iglesia and P. Stair for valuable discussions, A. Holmen for providing the exact dimensions of the monolith used in their studies of Pt-based catalysts and thank J. Moore for carrying out X-ray photoemission spectroscopy analysis of the Pt/AAO sample.

Additional information

Supplementary Information accompanies this paper on www.nature.com/naturematerials. Reprints and permissions information is available online at http://npg.nature.com/reprintsandpermissions. Correspondence and requests for materials should be addressed to S.V. or L.A.C.